Influence of the solidification microstructure and porosity on the fatigue strength of Al-Si-Mg casting alloys

I. Boromei[1], L. Ceschini[1], Al. Morri[1], An. Morri[1],
G. Nicoletto[2], E. Riva[2]
[1]University of Bologna, SMETEC Dept. - Bologna - Italy
[2]University of Parma, Dept. of Industrial Engineering - Parma - Italy

ABSTRACT

The fatigue behavior of Al-Si-Mg casting alloys is affected by the solidification microstructure and especially by defects such as gas pores, shrinkage pores and oxide films. This paper reports the microstructural characterization of a die cast engine head made of the A356 (G-AlSi7Mg0.3) alloy and the long-life fatigue strength determination using specimens extracted from the cast. The microstructural characterization was achieved by optical microscopy and digital image analysis to identify the different classes of solidification defects and to evaluate the correlation between local SDAS and the size and shape of the defects. Fatigue testing was performed under rotating bending and the stress amplitude vs cycles to failure dependence showed a large scatter. The reason for this is related to local stress concentration induced by the pores, which was analyzed by the finite element method, developing models of a material volume containing solidification pores characterized by 2D and 3D techniques (i.e. optical microscopy with image analysis and X-ray tomography, respectively).

RIASSUNTO

Il comportamento a fatica dei getti in lega Al-Si-Mg dipende in modo fondamentale dalla microstruttura di solidificazione ed, in particolare modo, dai difetti, quali pori da gas, cavità di ritiro e film di ossido. In questo lavoro è riportato la caratterizzazione microstrutturale di una testa motore in lega A356 (G-AlSi7Mg0.3) colata in conchiglia e la determinazione della resistenza a fatica su campioni estratti da getti. La caratterizzazione microstrutturale, effettuata con tecniche di microscopia ottica ed analisi di immagine, ha consentito di identificare le principali classi di difetti di solidificazione e di valutare eventuali correlazioni tra le dimensioni e la forma degli stessi e lo SDAS, dipendente dalla velocità di raffreddamento, anche locale, dei getti. La caratterizzazione a fatica è stata effettuata mediante prove a flessione rotante, determinando un'elevata dispersione del legame tra ampiezza di tensione e numero di cicli a rottura. Il comportamento è dovuto all'effetto dimensioni dei pori, come dimostrato dall'osservazione delle superfici di frattura in microscopia elettronica in scansione e da analisi col metodo degli elementi finiti, sviluppando modelli di un materiale contenente pori di solidificazione caratterizzato mediante tecniche 2D e 3D (cioè microscopia ottica con analisi delle immagini e tomografia a raggi X rispettivamente).

KEYWORDS

Al-Si-Mg alloys, fatigue, defects, X-ray tomography, finite element analysis
Acronyms. Optical Microscopy: OM; Image Analysis: IA; X-ray computer tomography: XCT; hot isostatic pressing: HIP; secondary dendrite arm spacing: SDAS; stress amplitude vs cycles to failure: S/N; stress concentration factor: K_t; Linear Elastic Fracture Mechanics: LEFM.

INTRODUCTION

The A356 alloy is a classic Al-Si-Mg casting alloy that can be age hardened by solution heat-treatment, quenching and aging (T6 condition). The A356-T6 alloy is widely used for the production of engine blocks and engine heads. There is a large amount of data in literature showing that the mechanical properties of Al-Si casting alloys are largely influenced by local microstructural features, which are strictly dependent on the chemical composition and local solidification conditions [1-10]. The casting process, in particular, inevitably introduces solidification defects, which can significantly reduce the mechanical properties and, above all, the fatigue strength of the final cast component, being elements of discontinuity and acting as stress concentrators. In the case of A356/A357 alloys, previous studies [5,6,11-14] have showed that among the solidification defects, gas porosity (typically spherical in shape), shrinkage cavities (of irregular and branched shape) and oxide films (bifilm) have a dominant effect on the fatigue behavior. The influence of these defects on the fatigue strength of the A356-T6 alloy was studied by Wang et al. [5] with repeated tests being carried out at fixed values of stress

amplitude. After grouping the test results with the same kind of defect as a fatigue crack initiator, the following important conclusions were obtained, [6]:

- porosity (without distinction between gas porosity and shrinkage cavities) is the defect that mainly affects fatigue life;
- only when the porosity is negligible (as in the case of castings subjected to hot isostatic pressing, HIP), the negative effect on the fatigue life of others solidification defects (such as oxide films) becomes appreciable. For example, the fatigue life of failed specimens with cracks nucleated at oxide films is 4-5 times longer than that of specimens failed by porosity;
- in defect-free specimens, the fatigue cracks generally nucleate at slip bands, eutectic Si particles and/or at intermetallic compounds. The resulting fatigue life is at least 25 times longer than that associated to cracks nucleated at pores.

The importance of reducing the size of defects, in particular casting pores, is clear and confirmed by all the literature data, which also show that when the size of the defect is reduced below a certain threshold, it does not correspond to an increase in fatigue life. The fatigue performance is directly related to the defect size and position: the greater the size and proximity to the free surface, the shorter the fatigue life of the component [11-15]. The concept of a failure-dominant pore (i.e. pore dominant for the initiation of cracks) that leads to fatigue failure is thus introduced.

Generally, the solidification defects mentioned earlier are almost always at least one order of magnitude larger than the microstructural constituents, thereby regulating the fatigue behavior of casting aluminum alloys. Only if their presence is negligible or their size comparable with that of the microstructural constituents, the latter may also influence the fatigue behavior of casting Al-Si alloys. The microstructural parameters that can mainly affect their fatigue behavior are: SDAS, size and shape of the eutectic Si particles and Fe-based intermetallic compounds [16-18].

This paper reports the results of microstructural characterization and fatigue testing carried out on specimens directly taken from different positions of engine heads, produced by gravity die casting with the A356 alloy. The microstructural characterization was aimed to identify the main classes of solidification defects and to assess any correlation between the size and shape of defects and the main microstructural parameters, which strongly depend on the local solidification conditions. The goal was to evaluate the negative influence of porosity on the fatigue strength of the A356 alloy, by performing an evaluation of the local stress concentration associated with this defect. This stress concentration was theoretically analyzed by the finite element method, developing models of a material volume containing solidification pores characterized by 2D and 3D techniques (i.e. OM with IA and XCT, respectively).

EXPERIMENTAL PROCEDURE

Microstructural analysis was carried out on A356 (G-AlSi7Mg0.3) specimens extracted from V8 engine heads, which were produced by gravity die casting. The alloy, which chemical composition is reported in Tab. 1, was refined with Ti-B, modified with Sr and degassed using a rotary lance degasser and high purity Ar. The casting was T6 heat-treated, solutioned at 535°C for 4.5 hours, water quenched and aged at 165°C for 4.5 hours.

The microstructural characterization was carried out by OM and IA in order to determine the SDAS and the following parameters related to the solidification defects: the percentage defects area fraction and some data related to the size and shape of the pore of maximum area, such as the equivalent diameter ($Deq=\sqrt{\frac{4 \cdot Area_{defect}}{\pi}}$), roundness ($R=\frac{[Perimeter_{defect}]^2}{4 \cdot \pi \cdot Area_{defect}}$) and Féret diameter (maximum size of a hypothetical rectangle surrounding the defect).

Table 1. Chemical composition of the A356 Al alloy (weight %)

Si	Mg	Fe	Cu	Mn	Zn	Ti	Sr	B	Al
7.24	0.42	0.138	<0.001	0.007	0.003	0.120	0.015	0.0354	Bal.

High cycle fatigue tests, using a reduced stair-case with test interruption at 10^7 cycles, were performed in order to quantify the role of pores on material strength and the predictive fatigue model, based on the mechanics of defects. Tests were carried out at room temperature, because the cylinder heads may experience fatigue failure of high number of cycles in areas of moderate temperature (i.e. less than 130°C). The type of specimen loading was rotating bending (at 50 Hz). The fatigue specimens were extracted from various parts of the engine heads. After the tests were completed, analysis of fracture surfaces was carried out by SEM, which confirmed the key role of large pores. The point of failure initiation was identified and both the critical pore size and distance from the free surface were determined.

To support an investigation of the effect of pore morphology on local stress concentration in the investigated alloy, two alternative techniques were used: i) OM; ii) XCT. The first technique determines the pore shape on a 2D section with fine spatial detail, the second one is a novel technique capable of reconstructing the 3D shape of a pore inside a small volume of material [19]. The XCT analysis of solidification pores was carried out at Elettra Synchrotron in Trieste. The digital reconstruction of the geometry of shrinkage cavities was carried out with in-house software [20]. The reconstructed pores were used to create finite element models of a material volume containing realistic porosity and to calculate the local stress state [21].

RESULTS AND DISCUSSION

CHARACTERIZATION OF MICROSTRUCTURE AND SOLIDIFICATION DEFECTS

The metallographic characterization of samples machined from the engine head, showed the typical solidification microstructure of a hypoeutectic Al-Si-Mg alloy, with dendrites of primary α-Al phase surrounded by the eutectic Al-Si. Solidification defects such as gas pores (basically round in shape) and interdendritic shrinkage cavities (irregularly shaped branches), were also detected. The OM and SEM micrographs, Fig. 1, did not show the presence of oxide film (i.e. bifilm).

The percentage area of defects and some parameters related to the shape and size of the largest defects (i.e equivalent diameter, roundness and Féret diameter), were evaluated with image analysis techniques, as described in Section 2. In this regard, microstructural analysis by OM can lead to an underestimation of the actual size of the defect, in relation to the position of the cutting plane for metallographic analysis compared to the actual defect [22]. For example, an optical micrograph of a shrinkage cavity section is shown in Fig. 2-a and XCT three-dimensional image, of the same type of defect, is reported in Fig. 2-b. Regarding the analysis of the defects, particularly low values of their percentage area (ranging from 0.02% and 0.34%) have been observed at the flame deck of the engine head. A critical area was, however, the central part of the cast, where the percentage reached the upper limit of about 1.5%, reflecting both the presence of sand cores and reduced feeding by the risers. Considering the value distribution of defects percentage area fraction and equivalent diameter, about 90% of the defect area values fall below 0.75% (Fig. 3-a) and about 90% of defects have a maximum equivalent diameter between 50 and 250 μm (Fig. 3-b).

Weibull charts were used to characterize the statistical dependence of pore size measurements obtained by metallography. This analysis, which can be used for estimation of the expected pore sizes in larger volumes of materials, showed that the two data set of percentage area fraction of defects (corresponding to lower and higher SDAS) are aligned (Fig. 4-a) following roughly a single Weibull distribution. This superposition of data, in the Weibull chart, demonstrates that SDAS value does not seem to affect the percentage area fraction of defects in the castings under investigation. The equivalent diameter data (Fig. 4-b) appear instead influenced by SDAS: lower values are found where SDAS is lower. Moreover the two set of data (corresponding to lower and higher SDAS) are not aligned in the chart, but follow two different Weibull distributions for values of D_{eq} lower or higher than approximately 100 μm, respectively. This trend can be related to a different genesis of the two classes of defects (with D_{eq} lower and higher than 100 μm, respectively). The presence of a threshold size below which the pore is not fatigue-critical was proposed in [13] and confirmed in [23]. Metallographic investigation is technically limited to a characterization of the porosity on restricted areas. However, thanks to a reference statistical distribution, as identified in Fig. 4b, the maximum pore

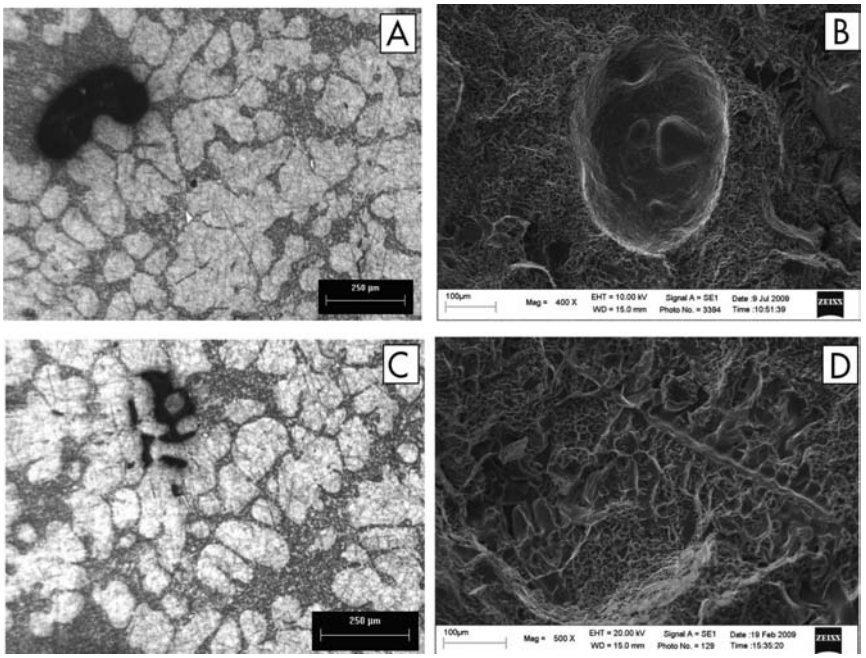

Fig. 1: Typical OM (a and c) and SEM (b and d) micrographs of gas pores and shrinkage cavities.

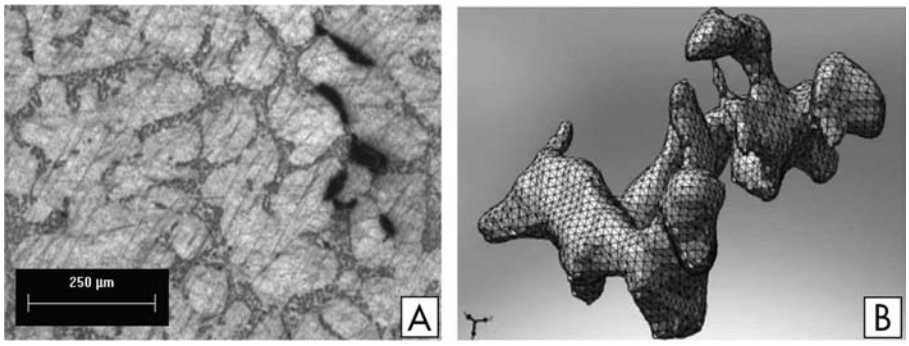

Fig. 2: Optical micrograph of a section of a shrinkage cavity (a) and a 3D image of the same type of defect obtained by XCT (b).

size expected in large section areas, with a direct link to fatigue strength, can be estimated [24].

It is well known that the mechanical properties of Al-Si alloy castings are also dependent on the values of SDAS. SDAS [μm] is directly related to the solidification rate (R [°C/s]), following the relationship: SDAS=k • R^m, where *k* and *m* are material constants (equal to 39.4 and -0.317, respectively, for alloy A356.). In the analyzed cast component, the minimum SDAS (30 μm) was found at the flame deck, where the solidification rate is higher due to the presence of suitable cooling systems, while the maximum SDAS value (70 μm) was measured in the central part, which is close to the sprue or surrounded by sand cores. The casting process simulation codes are able to determine the values of SDAS with high accuracy [25], while the prediction of the characteristics of the solidification defects can be more problematic. Correlations between the defect characteristics and SDAS were so investigated. The results, reported in the plots of Fig. 5, show the lack of correlation between SDAS and % area fraction of defects, as well as between SDAS and Féret diameter. Fig. 6a also shows the lack of correlation between the roundness and Féret diameter of the largest pores, while a reasonable correlation between Féret diameter and % area fraction of defects is shown in Fig. 6-b. Such a correlation, obtained by metallographic analysis, supports the use of simulation software for determining local defect size via % area fraction calculation. In addition, it is well known that fatigue behaviour of Al-Si cast components mainly depends on the size of the defects. For this reason, the existence of a correlation between Féret and % area fraction of defect should be useful in predicting the fatigue behavior of component.

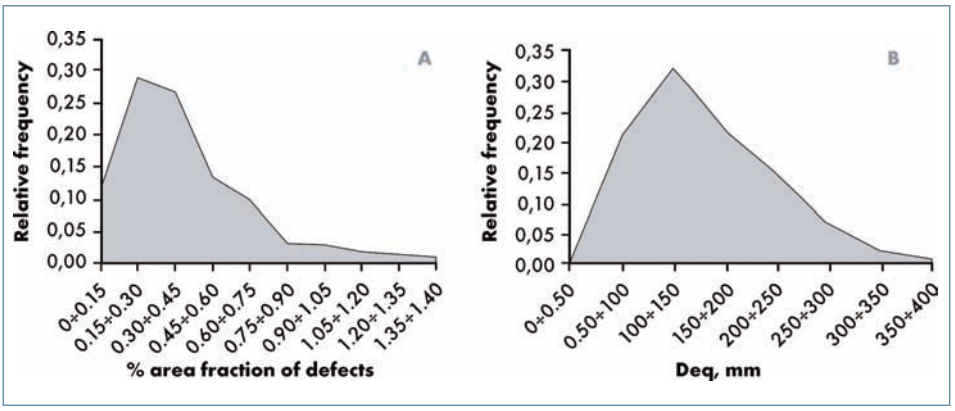

Fig. 3: Distributions of % area fraction of defects (a) and equivalent diameter of the largest pores (b) inside the cylinder head.

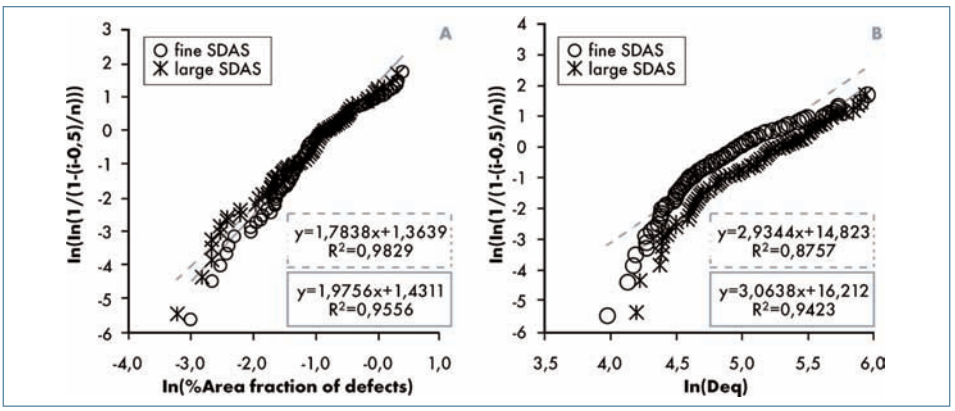

Fig. 4: Double parameter Weibull chart of % area fraction of defects (a) and equivalent diameter of the largest pores (b) for fine SDAS (<40 μm) and large SDAS (40-70 μm) zones.

FATIGUE BEHAVIOR IN THE PRESENCE OF DEFECTS

Data from rotating bending tests, on samples extracted from experimental castings and actual cast components, are presented in the S/N (stress amplitude vs cycles to failure) diagram of Fig. 7. Data points located at 10^7 cycles define multiple run-out, (i.e. specimens that reached the number of cycles without breaking). The scatter of fatigue life is the result of the presence of cast porosity in the A356 samples. The data scatter is large with min-max range of fatigue strength values at 10^7 cycles of 30 MPa - 75 MPa and an average value of fatigue strength of about 50 MPa. To quantify the role of the type of loading applied in long life fatigue test, push-pull tests were performed on broken specimens previously tested in rotating bending, [26]. The fatigue resistance in push-pull was found to be about 15% lower than in rotating bending due to the different material volumes under high stress.

SEM analyses of fracture surfaces confirmed the key role of porosity, which was always the point of fatigue crack initiation. Fig. 8 shows the pore of irregular shape, near the free surface of the sample, initiating the crack propagation. The crack propagated by taking a semi-elliptical shape up to the critical depth, which then led to the collapse.

MORPHOLOGY OF DEFECTS AND STRESS CONCENTRATION

The linear elastic fracture mechanics interpretation systematically includes the role of defects through the parameter K (stress intensity factor). K describes the elastic stress field at the tip of a crack and it is applicable when the crack length is considerably greater than the plastic zone size that inevitably forms at a crack tip in an elasto-plastic material. In addition to the nominal stress, K depends on the square root of crack length.

Recently, Shyam et al. [27,28] have interpreted the fatigue life initiated from a pore in a cast Al alloy as a small fatigue crack growth problem. He replaced the stress intensity factor range ΔK of the LEFM approach with a parameter that is the product of the monotonic and cyclic crack-tip displacements and the yield stress of the

material. He also demonstrated the applicability of the model to cast aluminum alloys over a wide range of experimental variables by conducting fatigue crack growth experiments from a micro-notch produced by pulse laser machining resembling a pore.

Independently of the approach, whether long or short crack, the scatter in results of the fatigue testing of cast AlSi alloy highlights the need to define the equivalent crack length of a pore. Therefore, an equivalent pore size $(Area)^{1/2}$, measured on micrographs, was proposed in [24] as the initial crack size and widely used for fatigue life calculations using the LEFM approach.

The $(Area)^{1/2}$ parameter, however, is insensitive to pore morphology.

When the pore is rounded (i.e. gas pore or non-metallic inclusions), its equivalent size is proportional to the radius. According to this definition, in case of elongated pores, such as a shrinkage cavity, the equivalent pore size, is much smaller than the Féret diameter. Moreover, the 2D micrographs often do not reveal the nature of typical tortuous and branched shrinkage cavity, as can be seen by comparing Figs. 2-a and 2-b.

The above issues have motivated studies based on the finite element method on the role of pore morphology as a response to high cyclefatigue life scatter. FEM models of microstructures and defects subjected to fatigue have been proposed [14, 29]. The analysis was carried out in the elastoplastic regime, since the phenomenon of fatigue damage is related to the development of microplastic deformation. The morphology of the porosity was defined by experimental evidence obtained by: i) OM and ii) XCT [19].

STATE OF STRESS AT DEFECTS CHARACTERIZED BY METALLOGRAPHIC ANALYSIS

Fig. 9 shows a typical shrinkage pore, whose area corresponds to equivalent size (A)1/2 = 88 μm. Initially, the analysis in the elastic range allows the stress concentration factor K_t to be determined, which is the ratio between local maximum stress and nominal stress. Fig. 10 shows the stress map around the pore loaded in a direction perpendicular to its maximum size leading to K_t = 8.8. Further investigation revealed that the K_t for shrinkage pores is always greater than 5, in some cases

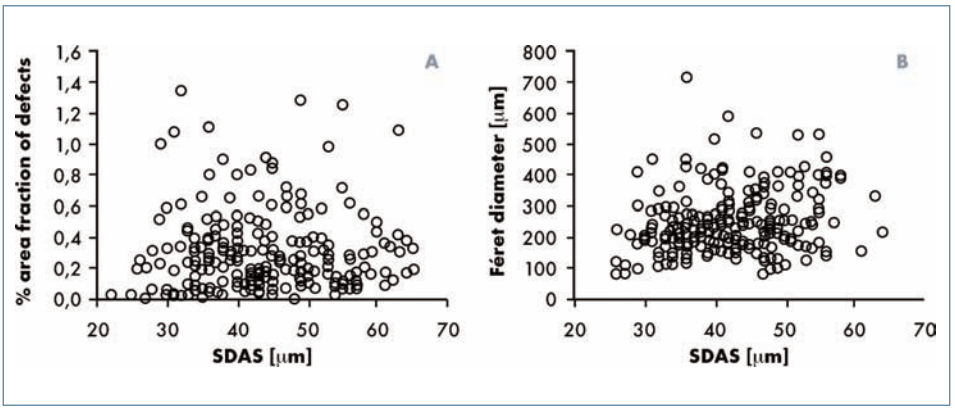

Fig. 5: Correlation between SDAS and % area fraction of defects (a), and between SDAS and Féret diameter (b).

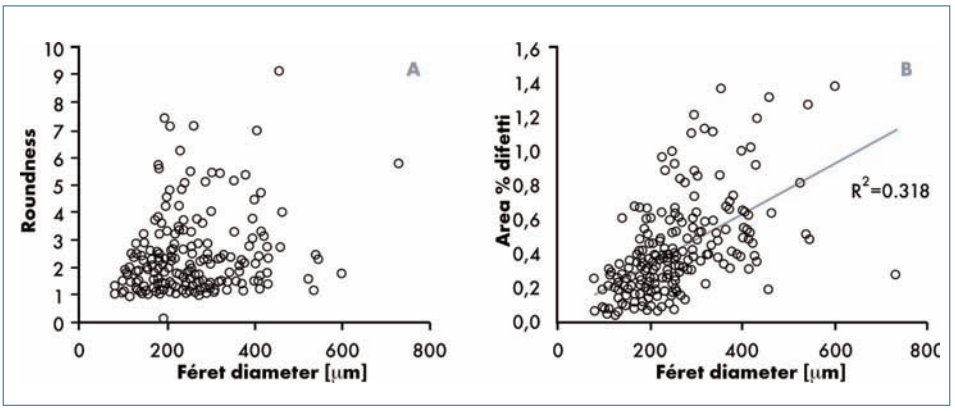

Fig. 6: Correlation between roundness and Féret diameter of the largest pores (a) and between Féret diameter and % area fraction of defects (b).

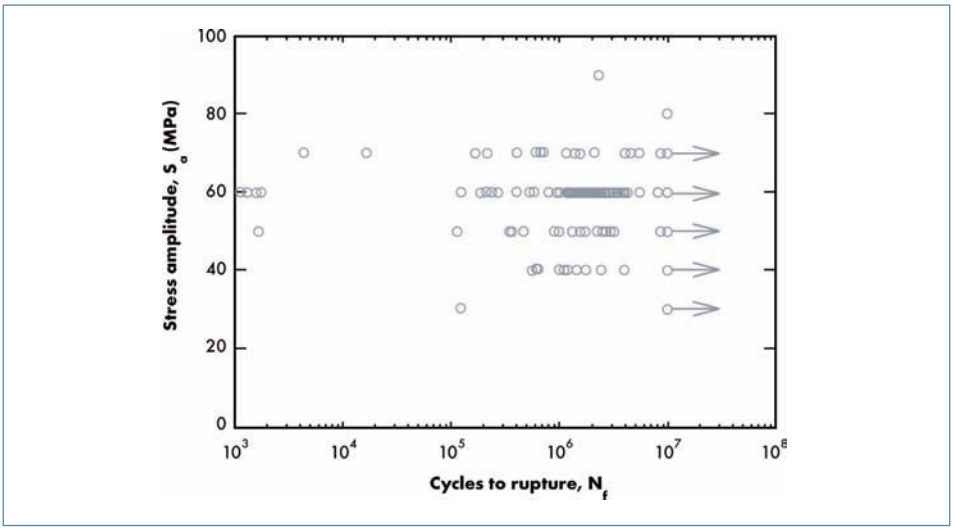

Fig. 7: S/N fatigue data for specimens extracted from several A356 gravity die cast components.

reaching values of 10. The high values of Kt show that the stress levels typical of high cycle fatigue (i.e. 40-60 MPa in fig 7), will always develop microplastic deformation at pores. Elastoplastic incremental analysis up to the nominal stress of 70 MPa, led to the development of the plastic zone at pore notches highlighted in Fig. 10. The same

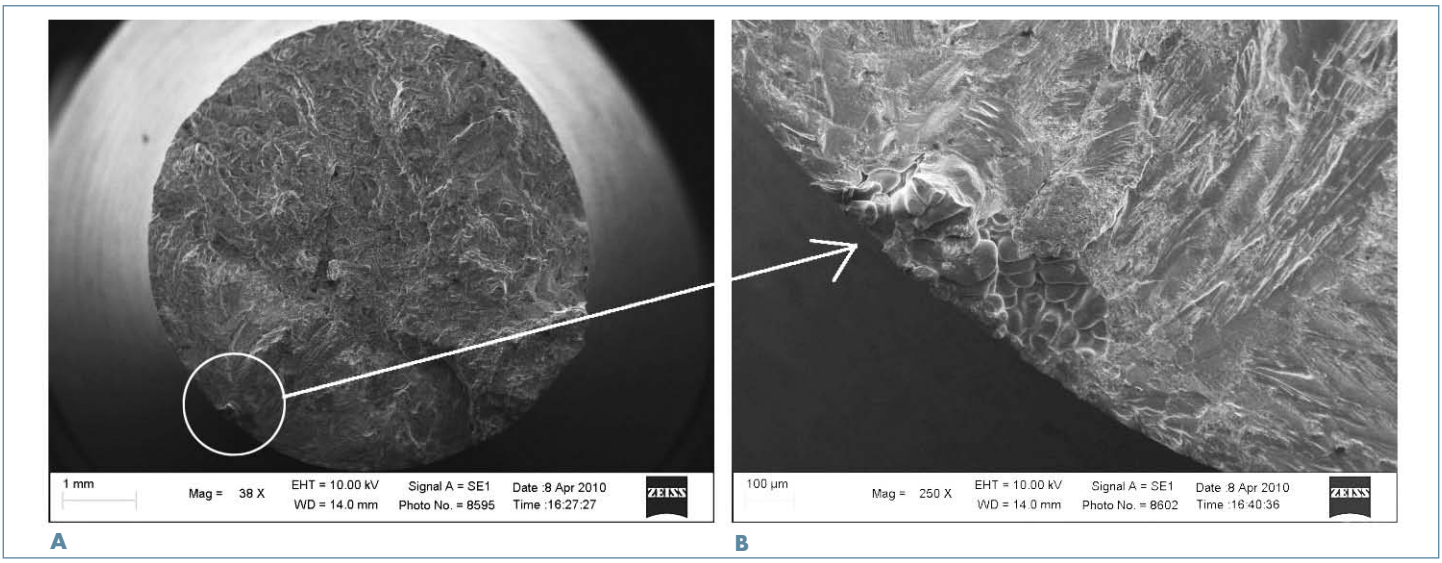

Fig. 8: Fracture surface of a fatigue specimen (a) and detail of the defect that initiated the crack (b).

image also shows the maximum pore size (Féret diameter) of almost twice the value of $(A)^{1/2}$. The morphology of the pore is very similar to a crack considered by fracture mechanics. Furthermore, the extension of the plastic zone was determined to depend non-linearly on the nominal stress, similar to models of elastoplastic fracture mechanics (i.e. for Cottrell Bilby Swinden (BCS)), [23].

STATE OF STRESS AT DEFECTS CHARACTERIZED BY X-RAY TOMOGRAPHY

A 3D reconstruction algorithm was developed to perform the tomography analysis of solidification defects, whose results were used to generate a finite element model of a volume of material with a microshrinkage cavity [21]. Fig. 11 shows the complex shape of the shrinkage pore reconstructed by XCT and the corresponding state of stress due to the application of a nominal stress of 70 MPa. The irregularities of the pore surface lead to strong fluctuations and local stress concentrations, as shown in Fig. 11. Maximum stress always develops in areas of minimum radius of curvature, calculated on any plane containing the direction of loading. It is reasonable to assume that this minimum curvature of the outer surface of a pore is related to the effect of surface tension of liquid alloy during the solidification process. Therefore, the formation of sharp edges is not possible. The average value of K_t for different pore orientations to the direction of load, was found to be equal to 3.2, with a variation of 15% in dependence of the orientation direction of loading. The K_t for a typical pore modeled in 3D is therefore lower than the values reported previously by 2D analysis. Figure 12 shows the accumulated plastic strain at nominally elastic stress of 70 MPa. A markedly three-dimensional effect is demonstrated with severe concentrations at points of maximum curvature of the pore surface.

CONCLUSIONS

This study confirmed the negative influence of porosity (cavity shrinkage and gas pores) on the fatigue strength of Al-Si casting alloys on the basis of: i) a comprehensive characterization of microstructural features and solidification defect on a cross-section of an A356 permanent mould cast engine head, ii) extensive fatigue testing on samples extracted from castings and iii) the stress analysis of casting defects. The following conclusions were reached:

- solidification conditions of the engine head are very different from area to area, leading to a variable microstructure, as shown by the local values of SDAS;
- porosity is not directly related to the local values of SDAS;
- large shrinkage pores promote the initiation of fatigue cracks, leading to premature failure of the samples with a high dispersion of data due to variability in the critical pore size;
- the damaging effect of a pore is related to local stress concentration, which was

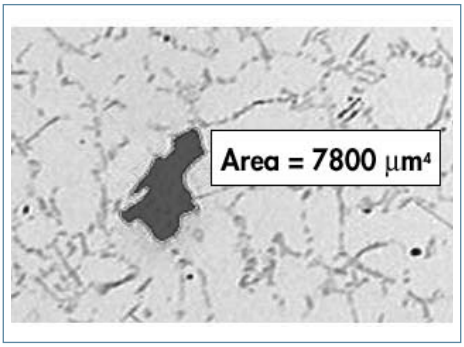

Fig. 9: Example of porosity observed by OM (2D): Area = 7800 µm2 , (A)1/2 = 88.3 µm

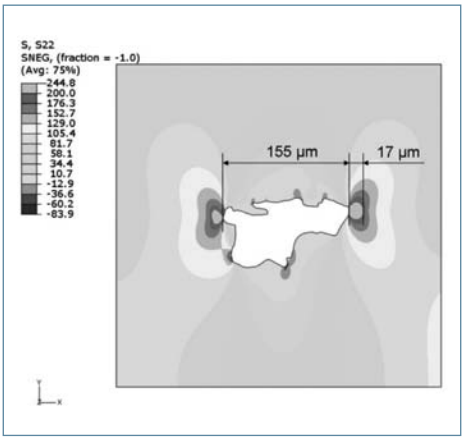

Fig. 10: Stress state around the 2D pore for a nominal stress of 70 MPa.

determined computationally for realistic shrinkage pores characterized with 2D (OM) and 3D (XCT) techniques.

ACKNOWLEDGEMENTS

The research was developed in the framework of the FAR project: "Study and design of mechanical components with high performance and reliability in aluminum alloys subjected to thermomechanical fatigue for engine applications". The authors wish to thank Dr. Gianluca Pivetti of Ferrari SpA, FAR project leader.

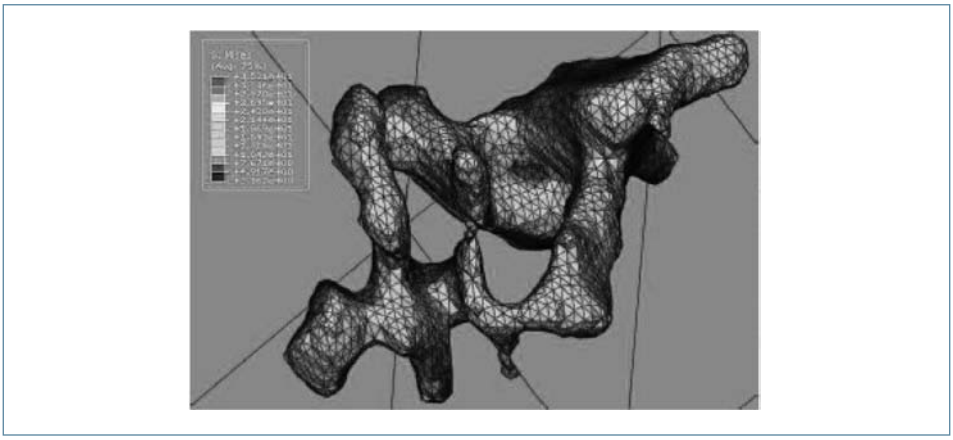

Fig. 11: Stress state around the 3D pore for a nominal stress of 70 MPa.

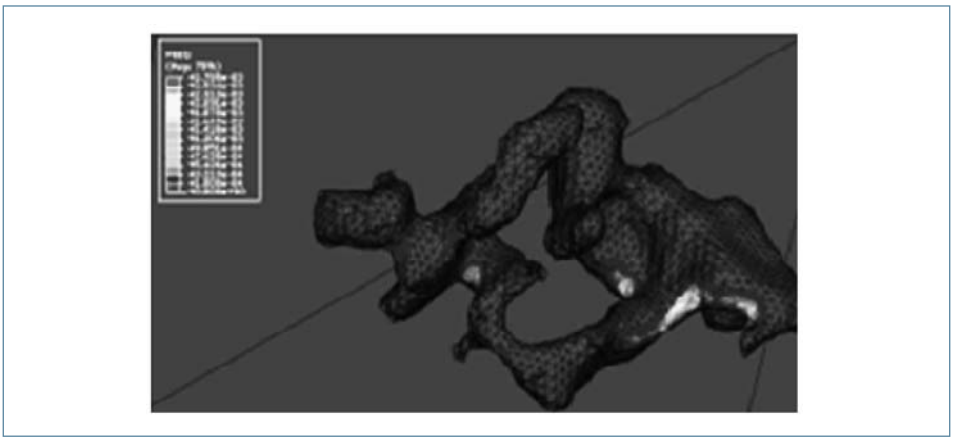

Fig. 12: Accumulated plastic deformation on pore surface for a nominal stress of 70 MPa.

REFERENCES

[1] N.D. Alexopoulos and S.G. Pantelakis. Mater Des, 25, 2004, pp. 419–430.

[2] D.A. Granger, R. Elliott,. Solidification of eutectic alloys: aluminum–silicon alloys, 9th ed,Metals handbook vol. 15, ASM International, Warrendale (PA);1988, pp. 159–181.

[3] M. Tiryakioglu, J. Campbell and J.T. Staley. Scripta Mater, 49,2003;, pp.873–878.

[4] C.D. Lee. Mater Sci Eng A, 464,2007;,pp. 249–254.

[5] Q.G. Wang, D. Apelian and D.A. Lados. J Light Met,1, 2001, pp. 73–84.

[6] J.Z. Yi, P.D. Lee, T.C. Lindley and T. Fukui. Mater Sci Eng: A, 432(1–2),2006, pp. 59–68.

[7] G.Ran, J. Zhou and Q.G. Wang. J Alloys Compd, 421(1–2),2006, pp. 80–86.

[8] L. Ceschini, Al. Morri and G. Sambogna. J Mater Process Technol, 204(1–3),2008, pp. 231–238.

[9] L. Ceschini, Al. Morri, An. Morri, A. Gamberini and S. Messieri. Materials & Design, 30, 2009, pp. 4525-4531.

[10] L. Ceschini, Al. Morri, An. Morri, G. Pivetti, Materials & Design, 32, 2011, pp. 1367-1375.

[11] J.Z. Yi, Y.X. Gao, P.D. Lee, H.M. Flower and T.C. Lindley. Met. Mater. Trans., 34A, 2003, pp. 1879-1890.

[12] M.J. Couper, A.E. Neeson and J.R. Griffiths. Fatigue Fract. Eng. Mater. Struct, 13, 1990, pp. 213-227.

[13] J.Y. Buffière, S. Savelli, P.H. Jouneau, E. Maire and R. Fougères. Mater. Sci. Engin. A,316, 2001, pp. 115-126.

[14] Y.X. Gao, J.Z. Yi, P.D. Lee and T.C .Lindley. Fatigue Fract. Eng. Mater. Struct, 27, 2004, pp. 559-570.

[15] J.Z. Yi, Y.X. Gao, P.D. Lee and T.C. Lindley. Met. Mater. Trans., 37B, 2006, pp. 301-311.

[16] Q.G. Wang, D. Apelian and D.A. Lados. J. Light Met., 1,2001, pp. 85-97.

[17] Q.G. Wang, C.H. Caceres and J.R. Griffiths. AFS Trans, 106, 1998, pp. 131-136.

[18] C.H. Caceres and J.R. Griffiths. Acta Mater., 44, 1996, pp. 25-33.

[19] E. Maire, J.Y. Buffiere, L. Salvo, J.J. Blandin, W. Ludwig and J.M. Letang. Adv. Eng. Mater.,3, 2001, pp. 539-546.

[20] G. Anzelotti, S. Fintová, R. Kone_ná, G. Nicoletto, 28th Danubia-Adria Symp, Mountanuniversitat Leoben, 2009, W. Eichlseder (Ed.), CD procs.

[21] G. Anzelotti, G. Nicoletto, A. Vincenzi, Procs. XXXVIII Convegno Nazionale AIAS, Politecnico di Torino, G. Belingardi and G. Curti (Eds.), AIAS, 2009, pp. 1-8.

[22] J.P. Anson, and J.E. Gruzleski, Mater. Character., 43, 1999, pp. 319-335.

[23] P. Baicchi, G. Nicoletto, E. Riva, R. Kone_ná, Procs. XXXVI Convegno Nazionale AIAS, Università di Napoli Federico II, R. Esposito (Ed.), AIAS, 2007, pp. 1-8.

[24] Y.Murakami, Metal Fatigue: Effects Of Small Defects And Nonmetallic Inclusions, 1st Edition, Elsevier, Oxford, 2002, pp. 321-330.

[25] R. Squatrito, I. Todaro, L. Tomesani, in: J. Campbell, P. Crepeau, M. Tiryakioglu (Eds.), Shape Casting: Third International Symposium, TMS, 2009, pp. 281-288.

[26] G. Nicoletto, R. Konecná, P. Baicchi, V. Majerova, Mater. Sci. Forum, Vol. 393-396, 2008, pp. 567-568.

[27] A. Shyam et al., Scripta Mater. 50, 2004 pp. 1109–1114.

[28] A. Shyam A., E. Lara-Curzio, Inter. J. Fatigue, 32, 2010, pp.1843–1852

[29] D.L. McDowell, K. Gall, M.F. Horstemeyer, and K. Fan., Eng. Fract. Mech.,70, 2003,pp.49-80.